STRESSES NEAR A HOLE IN A TUBE UNDER TORSION

LUTHER EUGENE MAYES

1953

STRESSES NEAR A HOLE IN A TUBE UNDER TORSION

-

L. E. Mayes

STRESSES NEAR A HOLE IN A TUBE UNDER TORSION

by

Luther Eugene Mayes,
Lieutenant, United States Navy

Submitted in partial fulfillment
of the requirements
for the degree of
MASTER OF SCIENCE
in

MECHANICAL ENGINEERING

United States Naval Postgraduate School
Monterey, California
1953

This work is accepted as fulfilling
the thesis requirements for the degree of
MASTER OF SCIENCE
in
MECHANICAL ENGINEERING

from the
United States Naval Postgraduate School

PREFACE

This thesis evolved in the mechanical engineering laboratory at the U. S. Naval Postgraduate School, Monterey, California. Upon the sight of a finite plate containing a hole which was set up in a tension experiment, the idea was entertained that if the sides of the plate were bent around in a circular arc and welded together, a hollow shaft or tube containing a hole would result, - more important and intriguing (or so it seemed at the time) was its imagined relation to an infinite plane. When a check of the literature brought no discussion on this particular problem to light, the project of determining experimentally just how the stresses behaved in this tube under a torque load was adopted. It was carried out between March and May, 1953, in the laboratory mentioned above.

The writer takes this opportunity to express a profound appreciation to Professor Robert E. Newton for his extremely valuable contribution of overall guidance. It is further desired to acknowledge the gratitude felt toward Wayne E. Bird, Ph3, USN, who did the photographic work which appears in the thesis.

TABLE OF CONTENTS

CHAPTER TITLE PAGE

Preface ii

List of Illustrations v

Table of Symbols vii

Summary 1

I An Introduction to the Problem

1. Statement of the problem 2

2. Nature of the state of stress for a tube with a single hole 2

3. The tube with two holes and its associated plane problem 3

4. Background of previous work bordering on the plane problem 5

5. The tube with a single hole 5

6. The three-dimensional nature of the tube problem 6

II Equipment and Technique Employed

7. Tube material 7

8. Method of perforating tubing 7

9. Strain gage selection 7

10. Stresscoat treatment 8

11. Loading of test specimen 9

12. Experimental technique 9

13. Significance of use of AX-5 gages 9

III Reduction of Data

14. Transverse sensitivity corrections 11

15. Method employed in determining strain concentration curves 11

CHAPTER TITLE PAGE

16. Law of failure for Stresscoat 11
17. Use of strain gages for calibration of crack patterns 12

IV The Results

18. The presentation of results 13
19. Interpretation of results 27
20. Similarities to the Kirsch problem 28

V Major Sources of Error

21. Loading error 30
22. Uncertainties inherent in Stresscoat tests 30
VI Conclusion 32
Bibliography 33
Appendix I: Strain Concentration vs. r/a Along the Line $\theta = 25°$ For a Tube with a Hole Size, $a/b = 0.106$ 35
Appendix II: Proof that the Tube with a Single Hole has no Analogue among the Plane Problems 36

LIST OF ILLUSTRATIONS

Figure	Title	Page
1	Tube with a Single Hole under Torsion	2
2	Tube with Two Holes and Associated Plane Problem	3
3	Developed Tube Surface Containing Two Holes	4
4	Stress Concentration vs. r/a Along the Line $\theta = 0^\circ$	14
5	Stress Concentration vs. r/a Along the Lines $\theta = 5^\circ$, 15°, 25°, and 35° for a Tube with a Hole Size, $a/b = 0.106$	15
6	Stress Concentration vs. r/a Along the Lines $\theta = 45^\circ$, 55°, 65°, 75°, 85°, and 90° for a Tube with a Hole Size, $a/b = 0.106$	16
7	Typical Isoentatic Distribution on the Developed Surface of a Tube with a Hole Size, $a/b = 0.106$	17
8	Stresscoat Crack Pattern for $a/b = 0.0585$ (Side View)	18
9	Stresscoat Crack Pattern for $a/b = 0.0585$ (Top View)	19
10	Stresscoat Crack Pattern for $a/b = 0.106$ (Side View)	20
11	Stresscoat Crack Pattern for $a/b = 0.106$ (Top View)	21
12	Streascoat Crack Pattern for $a/b = 0.202$ (Side View)	22
13	Stresscoat Crack Pattern for $a/b = 0.202$ (Top View)	23
14	Stresscoat Crack Pattern for $a/b = 0.23$ (Side View)	24
15	Stresscoat Crack Pattern for $a/b = 0.23$ (Top View)	25
16	Stress Concentration on Inner and Outer Tube Surfaces vs. r/a Along the Line $\theta = 0^\circ$ For a Hole Size, $a/b = 0.23$	26

LIST OF ILLUSTRATIONS

Figure	Title	Page
17	Strain Concentration vs. r/a Along the Line $\theta = 25^\circ$	35
18	Right Circular Cross-section of Tube Taken on a Plane through the Center of the Hole	36

Table No.	Title	Page
1	Maximum Stress Concentrations	13
2	Comparison of Stresscoat and Strain Gage Data	31

[illegible]

[illegible]	[illegible]	[illegible]
[illegible]	[illegible]	[illegible]
[illegible]	[illegible]	[illegible]

[illegible]	[illegible]	[illegible]
[illegible]	[illegible]	[illegible]
[illegible]	[illegible]	[illegible]

INDEX OF SYMBOLS

$\sigma_1, \sigma_2, \sigma_3$	Principal stresses, $\sigma_1 \geqslant \sigma_2$, $\sigma_3 = 0$.
σ_∞	Tensile principal stress (σ_1) in undisturbed portion of the tube (not near the hole).
τ	Shearing stress.
τ_∞	Shearing stress in undisturbed portion of tube.
$\epsilon_1, \epsilon_2, \epsilon_3$	Principal strains corresponding to the principal stresses.
ϵ_∞	Tensile principal strain in undisturbed portion of tube.
a	Radius of the hole.
b	Distance between hole centers measured around the circumference of the tube.
R	Mean radius of tube $\left(\frac{\text{outer radius} + \text{inner radius}}{2}\right)$.
r	Radial distance on the developed tube surface measured from the center of the hole.
θ, ϕ	Angles.

SUMMARY

This thesis describes and reports the results of an experimental determination of the principal stresses near a hole (a circle on the developed surface) in a thin-walled tube under torsion. Four tubes of $1\frac{1}{2}$" o.d., 0.050" wall thickness, 24S-T aluminum alloy were used in the investigation; two of the tubes contained but a single hole ($a/b = 0.0585, 0.106$, where a/b refers to the ratio of hole radius to distance between hole centers around the circumference of the tube); the others contained two holes centered diametrically opposite one another ($a/b = 0.202, 0.23$).

Brittle lacquer (Stresscoat) and resistance wire strain gages served as tools for the conduct of the investigation. A few type A-7 strain gages were spotted at strategic locations to confirm information rendered by tests with Stresscoat.

Curves of stress concentration at various locations around the hole are shown for four ratios of a/b. Photographs of Stresscoat crack patterns, indicating the principal stress trajectories, are also included. Although it had been initially anticipated that the tube problem possessed a plane analogue, results indicated that this was not true.

CHAPTER I

AN INTRODUCTION TO THE PROBLEM

1. Statement of the problem.

This thesis is a report of an experimental determination of the stresses in the neighborhood of a hole in a thin-walled tube under torsion.

2. Nature of the state of stress for a tube with a single hole.

A thin, hollow, circular shaft or tube under torsion is theoretically in the two-dimensional state of stress known as pure shear where the principal stresses, σ_1, σ_2 and σ_3 take on the relations $\sigma_1 = -\sigma_2$; $\sigma_3 = 0$. (The convention that σ_1 is the algebraically greater stress is adopted in this report, i.e., $\sigma_1 \geqslant \sigma_2$.) If a hole is drilled through one surface of the tube, considerable variation in the principal stress components occurs in areas near the hole. At large distances from the hole, the condition of stress is one of pure shear; near the hole, lines emanating from the center of the hole in the directions θ = 0°, 90°, 180°, 270° are lines along which pure shear also exists. σ_1 at any particular point in one quadrant around the hole is equivalent to minus σ_2 in the corresponding image point in an adjacent quadrant.

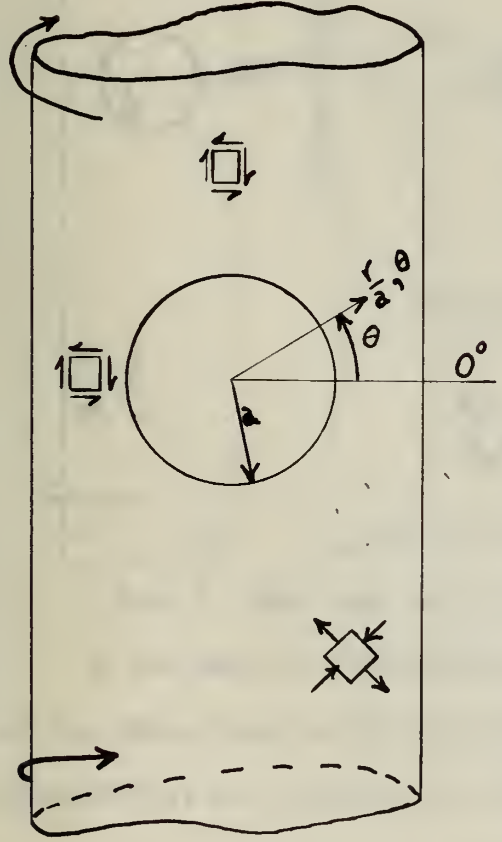

Fig. 1 Tube with a Single Hole under Torsion

Thus, the state of stress over the entire surface of the tube is one of anti-symmetry. This characteristic makes the use of brittle lacquer exceptionally well adapted for quantitative measurements of strain and through them, the computation of principal stresses involved. An analysis need only be carried out over 180° around the hole, or over two adjacent quadrants, and the coupling of strains obtained yields solutions for the principal stresses all around the hole.

3. The tube with two holes and its associated plane problem.

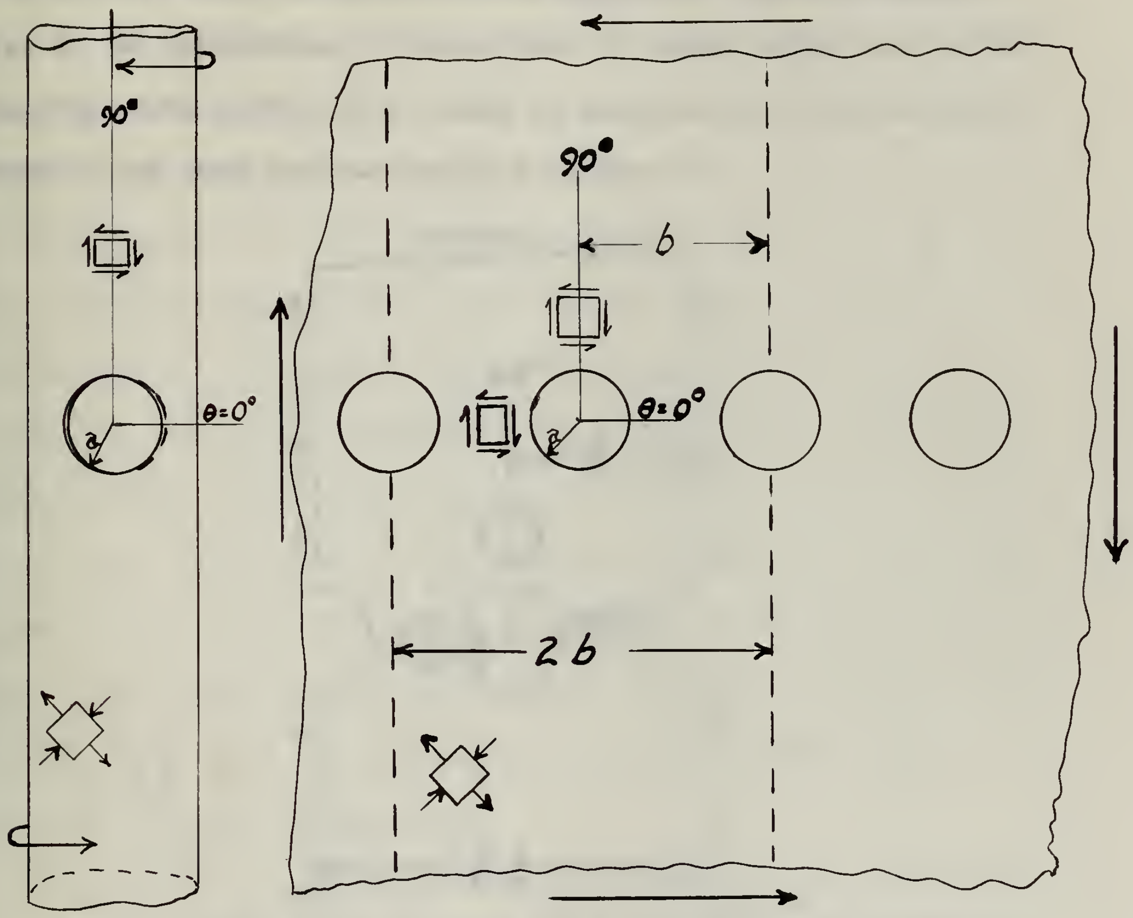

Fig. 2 Tube with Two Holes and Associated Plane Problem.

If the hole is drilled through both the top and bottom surfaces of the tube, this particular problem may be further analyzed and presented as an extension or a variation of Kirsch's problem. The

tube containing the holes is closely related to an infinite plate containing an infinite series of holes located on the 0°-180° axis at a distance apart equal to half the circumference of the tube. Fig. 2 shows the tube and its associated plane problem, the stresses of which are likewise anti-symmetric in character. If the tube is laid out as a developed surface, it can be represented in the manner shown in Fig. 3. It can be seen that the developed surface shown in Fig. 3 can equally well be represented in the dashed lines in Fig. 2. Or conversely, if the portion in dashed lines were lifted from the plate in Fig. 2, it would be assigned shear forces attributed to the developed tube section in Fig. 3.

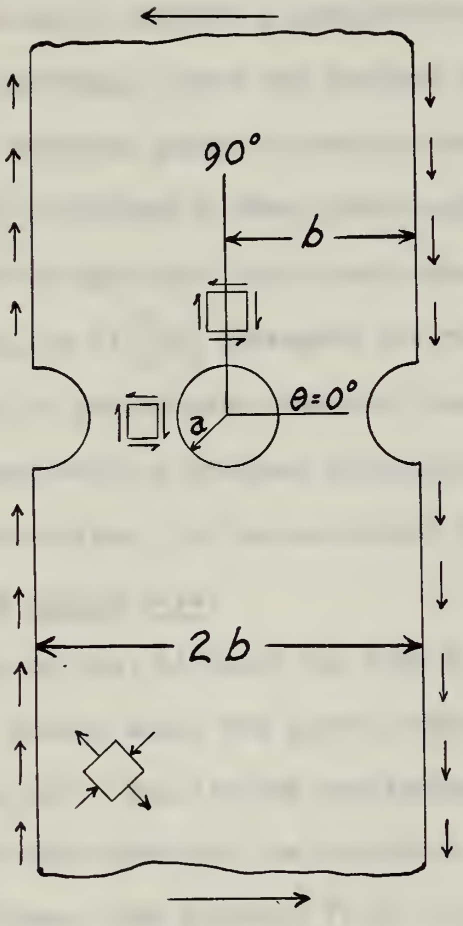

Fig. 3 Developed Tube Surface Containing Two Holes.

4. Background of previous work bordering on the plane problem.

Although variations of the Kirsch problem have provided an unusually fertile field for numerous investigators, a reasonably thorough search of the literature by the writer disclosed no theoretical solution for this particular variation. Howland and Knight [4] described in detail the tactical procedure to be followed in one method of attack. It would lead to a theoretical solution to this plane problem after many quite tedious computations. The authors carried out the necessary computations for several cases in which the physical configurations of the plates were similar to that in Fig. 2, but a symmetric condition of loading was chosen in each case in order that the stresses could be represented by even functions and to simplify the problem. Since the loading in this problem is anti-symmetric, the stresses assume expression in terms of odd functions. Wang [12] developed a theoretical solution for the anti-symmetric case of the single hole in a finite square plate loaded by pure shear. Ruffner, et al [10] presented the results of an experimental determination by photoelastic means of the problem treated by Wang. These represent work on problems which are the closest approximations, known to the writer, to the associated plane problem.

5. The tube with a single hole.

It should be noted that although the tube with the two holes possesses a distant cousin among the plane problems, the tube with the single hole does not. Equilibrium conditions along the line $\theta = 0^\circ$ impose restrictions which preclude the existence of a counterpart among the plane problems (see Appendix II for further amplification).

This fact was not realized until insufficient time remained to exploit the knowledge fully. From the first, it had been anticipated that the tube with the single hole was indeed analogous to an associated plane problem, and the experimental program was designed accordingly.

6. The three-dimensional nature of the tube problem.

The process by which torque is carried in a closed, circular, thin-walled tube involves shearing stresses which are substantially constant through the thickness of the tube wall. A tube with a longitudinal slit, however, behaves in a manner much like the developed sheet loaded in torsion (not pure shear), where the sheet is actually twisted, not merely distorted in its own plane. In the present problem, the hole functions locally as a longitudinal slit. It was found that both phenomena were present in the vicinity of the hole. This was confirmed by the nature of the crack pattern of the brittle lacquer, by equilibrium checks, and by strain gage data obtained from the inside surface of the tube.

CHAPTER II

EQUIPMENT AND TECHNIQUE EMPLOYED

7. Tube material.

The desirable features of a favorable modulus of elasticity and a relatively long range linear stress-strain relationship led to a choice of aluminum alloy 24S-T seamless tubing. Availability limitations restricted the tubing size to $1\frac{1}{2}$" o.d. and 0.050" wall thickness. Tube lengths of two and three feet were selected to facilitate handling of the test pieces.

8. Method of perforating tubing.

Investigations were undertaken for four values of the parameter a/b; two of the tubes contained but a single hole (a/b = 0.0585, 0.106); the other two (a/b = 0.202, 0.23) had two holes centered diametrically opposite one another. The holes were initially drilled in the sections of tubing with an undersize drill; they were subsequently filed to obtain edges which were normal to the surface and of the proper profiles - circles on the developed surfaces. To transfer the profile to the tubing, templates were cut out of paper, and the paper was wrapped around the tubing to permit scribing of the profile on the tube surface.

9. Strain gage selection.

An SR-4 type AX-5 resistance wire gage was cemented on each test section sufficiently distant from the hole along the longitudinal axis of the tube such that it would measure the principal strains present on the surface of the undisturbed portions of the tube, where a uniform condition of pure shear prevailed. The size of the tube precluded the

use of rosette gages in the disturbed regions around the hole, and it prompted the use there of A-7 type gages with grid dimensions of 0.1" x 0.25" to the exclusion of other types. The A-7 gages were used to confirm data contributed by tests with Stresscoat, the type of brittle lacquer commercially available. An attempt was made to select locations for the A-7 gages where the gradient of strain was not too large and where the condition of stress was that of pure shear, although the stipulation of pure shear was not really necessary, since an analysis of the information yielded by Stresscoat provides the proper orientation and relative magnitudes of the principal strains at any point on the surface of the tube.

10. Stresscoat treatment.

Stresscoat was sprayed on the test sections in the open air outside the laboratory. The Stresscoat on a section of tubing and the accompanying calibration strips were dried either in the laboratory at uncontrolled room temperatures or in a cabinet which offered a temperature of approximately 90°F. A minimum drying time of 6 hours was imposed on specimens placed in the cabinet; those dried at room temperature were allotted 18 to 24 hours for drying.

Four calibration strips were used with each test. One calibration was made at the start of the test to determine the initial loading for the test specimen. Another calibration was made when cracks had progressed to the location of a confirmation gage. The third was used in an intermediate stage of the test when it was felt necessary, since neither temperature nor humidity was controlled during tests, and, at times, they varied widely. The fourth was used at the conclusion of the test. The calibration strips were loaded rather

rapidly in, as nearly as possible, an identical manner; the time consumed in applying the load was less than one second.

11. Loading of test specimen.

The test specimens were loaded in a standard Tinius-Olson Torsion Tester on the 0 to 12,000 pound-inch scale, but actual loading covered only 0 to 1,200 pound-inches. The twisting rate was maintained at 20° per minute, and the loading was controlled by push buttons. The creep correction chart provided in the Stresscoat instruction book permitted a correlation between discrepancies in loading times for calibration strips and test specimen and accounted for the influence of creep of the brittle lacquer on the test specimen.

12. Experimental technique.

Polar grids were drawn on cellophane with a wax pencil and on cellulose acetate with India ink. These were wrapped around the coated tube to permit rapid identification of cracks as to orientation and location. The crack pattern was sketched on a separate polar plot as the cracks developed; sketches of cracks occurring with each loading increment were colored differently to enable proper identification in later analyses. Approximately four loadings per hour allowed enough time to sketch new cracks and permit the coating to recover between loadings. The tube was loaded to the desired torque, torque and strain gage data recorded, and the torque was removed while the lacquer recovered and cracks were sketched.

13. Significance of use of AX-5 gages.

Data taken from the AX-5 strain gage was treated as the primary loading reference, since through its indicator unit, it measured the

principal strains in the undisturbed portion of tubing. A strain, corresponding to the desired loading, was set on the strain indicator, and torque was applied until the desired strain had been reached. The AX-5 strain gage was connected as its own active and compensating gage; this doubled the response and more nearly eliminated drift due to changing temperature conditions.

CHAPTER III

REDUCTION OF DATA

14. Transverse sensitivity corrections.

For the AX-5 gages, a transverse sensitivity of 1/30 (recommended by the manufacturer) was used in correcting apparent strain to true strain. Dohrenwend and Mehaffey, as reported by Hetenyi [5], confirm the 1/30 figure and also give the transverse sensitivity correction to be applied to A-7 gages (-0.01).

15. Method employed in determining strain concentration curves.

The principal strain concentration ($\frac{\epsilon_1}{\epsilon_\infty}, \frac{\epsilon_2}{\epsilon_\infty}$) at any point in the region near the hole was obtained by dividing the value of the threshold of strain sensitivity of the brittle lacquer by the tensile principal strain (ϵ_∞) which existed in the undisturbed regions. It is clear that the actual strain concentration could lie between values indicated by the cracks at a particular load and the preceding load, because the crack could have been formed at any value between successive loads. Accordingly, two sets of values of strain concentration were plotted versus the parameter r/a (ratio of radial distance on the developed surface from the center of the hole to the radius of the hole) at each point where Stresscoat data were obtained, and a curve of strain concentration versus r/a was drawn between boundaries defining the sets. A representative plot is shown in Appendix I to indicate the relative spread and reproducibility of data.

16. Law of failure for Stresscoat.

From the values of $\frac{\epsilon_1}{\epsilon_\infty}$ and $\frac{\epsilon_2}{\epsilon_\infty}$ at any point, $\frac{\sigma_1}{\sigma_\infty}$ and $\frac{\sigma_2}{\sigma_\infty}$, principal stress concentrations, were computed from Hooke's law for

two-dimensional stress. Due regard was accorded information set forth by Durelli and DeWolf [1] ; however, correlations between strain gage data and Stresscoat data in these experiments seemed to bear out the established law, based on the maximum strain theory, for failure of Stresscoat rather than that proposed by Durelli and DeWolf.

17. Use of strain gages for calibration of crack patterns.

During some of the tests performed on the tube with an a/b ratio of 0.106, calibration strips were placed on an adjacent cabinet housing electronic circuits of the torsion tester. It was found that after long periods of operation, the cabinet became heated to the extent that calibrations taken from the strips at the conclusion of the test no longer reliably predicted the threshold of strain sensitivity on the coated tube. Strain gage data was used for calibrating the Stresscoat pattern at low concentrations of strain on these particular tests (see Table 2). In every other instance, strain gage data merely provided substantiating information to Stresscoat data.

CHAPTER IV

THE RESULTS

18. The presentation of results.

Numerical results obtained from tests are shown graphically in Figs. 4, 5, 6, and 16, where stress concentrations are plotted against the parameter r/a. Fig. 4 offers a graphical comparison of stress distributions along the line $\theta = 0^\circ$ between the various a/b ratios. A detailed exploration of the state of stress was undertaken on the tube containing the single hole with an a/b ratio of 0.106. The distribution of stresses was determined at 5° intervals around the hole, but in the presentation of these data, in Figs. 5 and 6, the interval was increased to 10°. Fig. 7 illustrates the characteristic appearance of a polar plot of isoentatics for the case in which a/b = 0.106. In order to furnish a more complete picture, photographs showing two views of the Stresscoat crack patterns which were obtained for each tube are included in Figs. 8 through 15.

The location and numerical value of the maximum stress concentration which developed in each case is given below in Table 1.

TABLE 1

MAXIMUM STRESS CONCENTRATIONS

a/b	Location		$\frac{\sigma_1}{\sigma_\infty}$ Stress Concentration
	r/a	θ	
0.0585	1.6	-25°	3.2
0.106	1.35	-25°	7.9
0.202	1.1	-30°	10.5
0.23	1.15	-35°	11.6

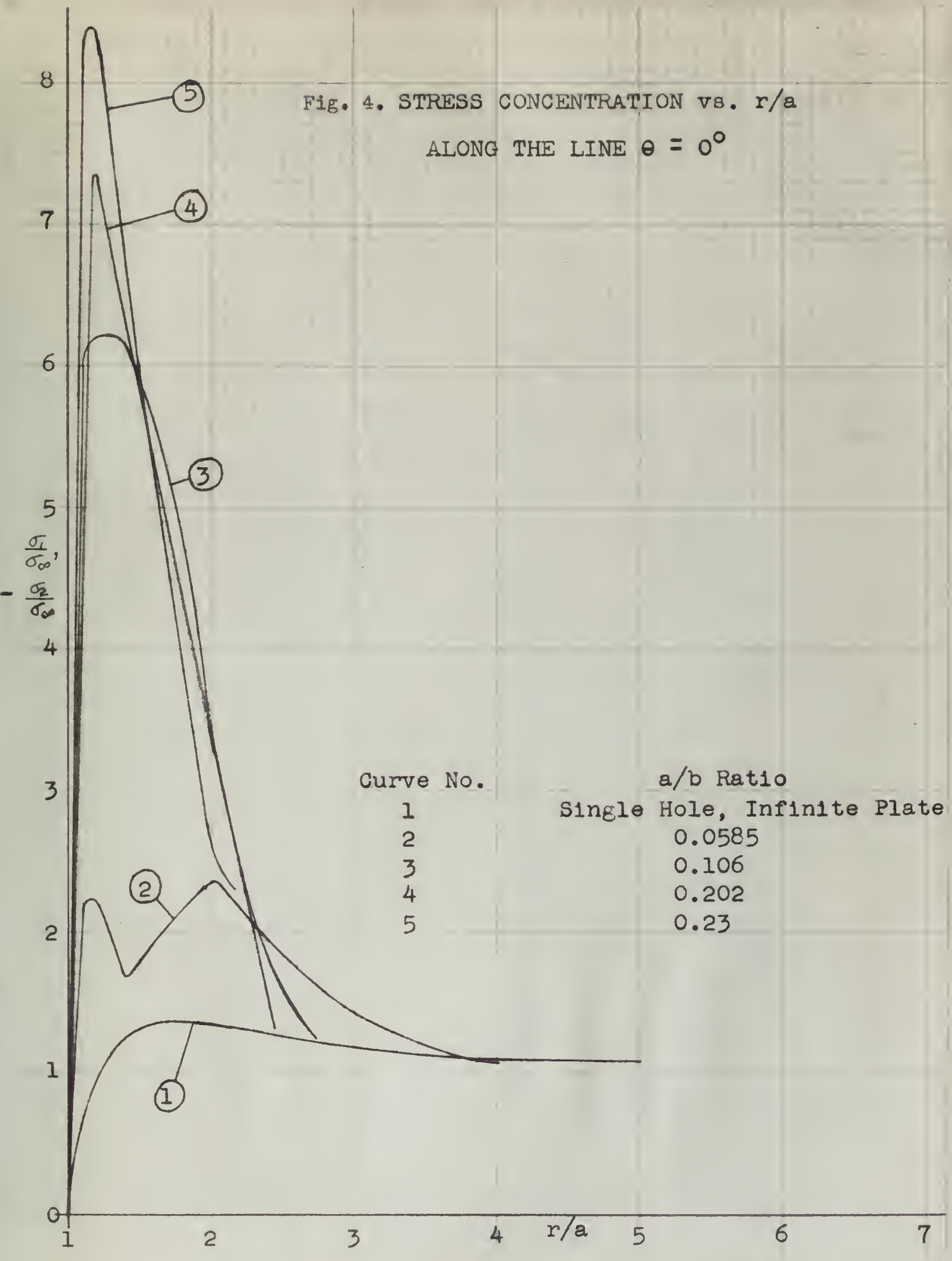
Fig. 4. STRESS CONCENTRATION vs. r/a

ALONG THE LINE θ = 0°

Curve No.	a/b Ratio
1	Single Hole, Infinite Plate
2	0.0585
3	0.106
4	0.202
5	0.23

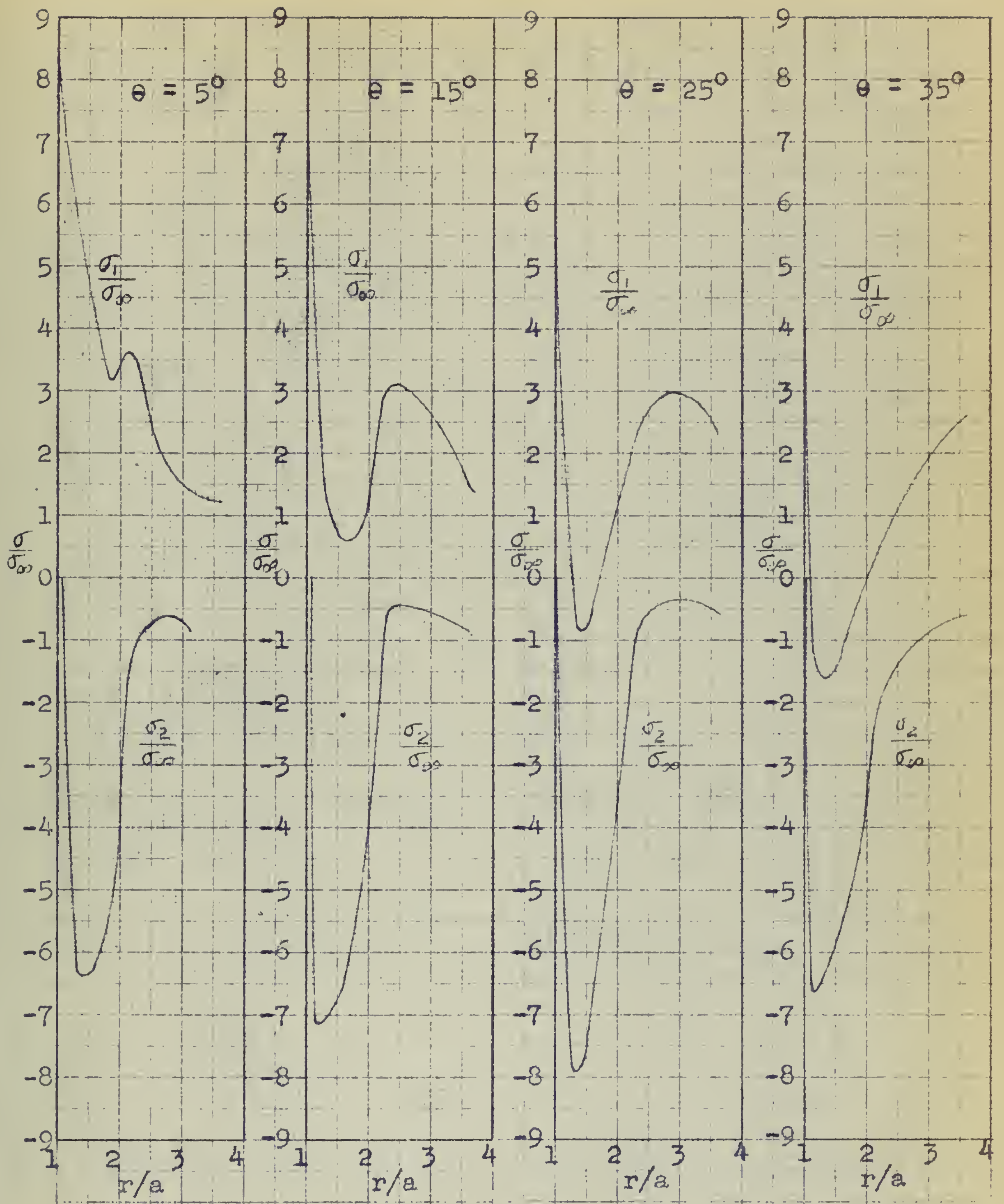

Fig. 5 STRESS CONCENTRATION vs. r/a ALONG THE LINES θ = 5°, 15°, 25°, AND 35° FOR A TUBE WITH A HOLE SIZE, a/b =0.106

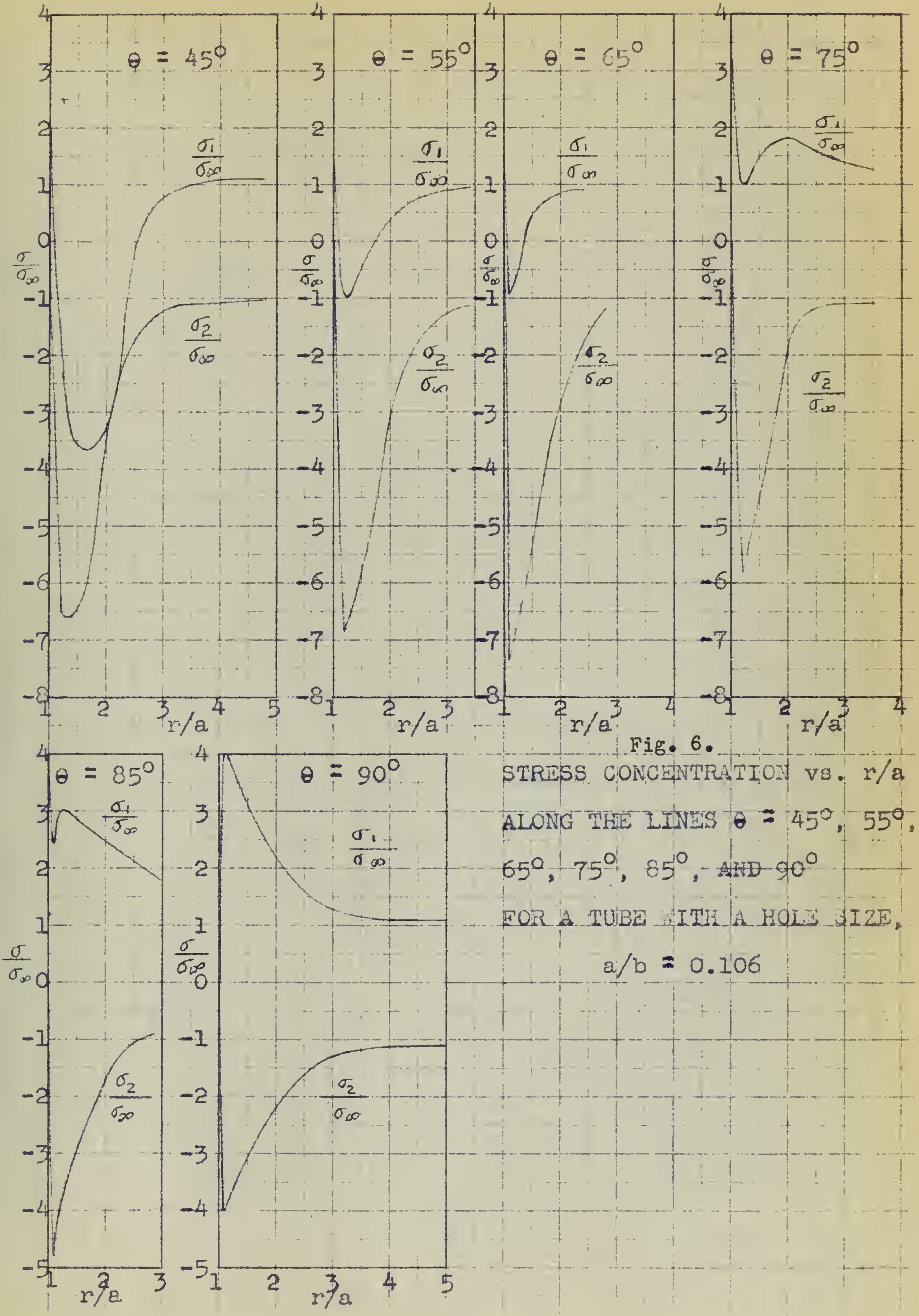

Fig. 6.

STRESS CONCENTRATION vs. r/a ALONG THE LINES θ = 45°, 55°, 65°, 75°, 85°, ~~AND~~ 90° FOR A TUBE WITH A HOLE SIZE,

a/b = 0.106

Fig. 7 Typical Isoentatic Distribution on the Developed Surface of a Tube with a Hole Size, a/b = 0.106

Load No.	Torque, lb-in
1	200
2	300
3	400
4	500
5	600
6	900

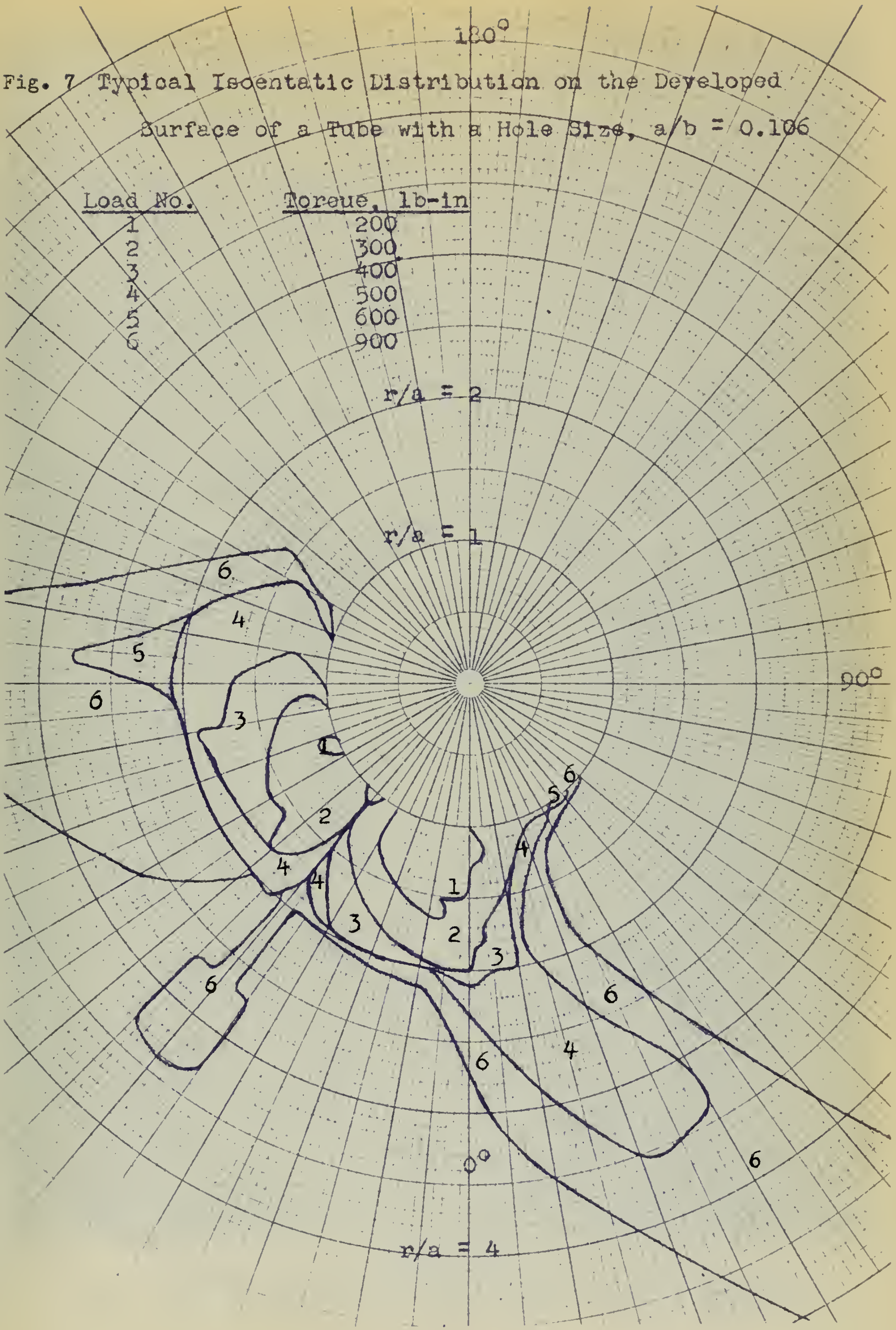

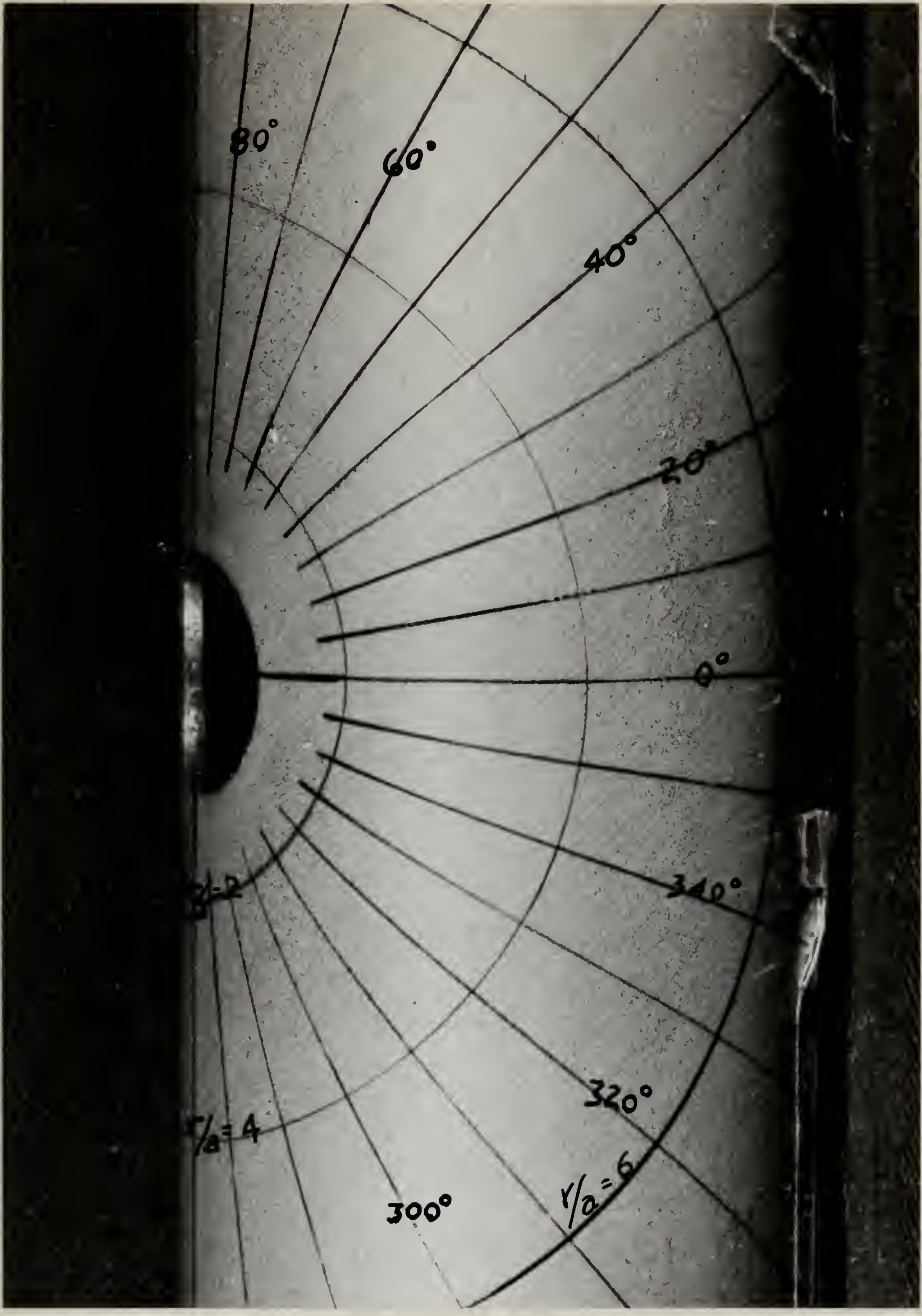

Fig. 8 Stresscoat Crack Pattern for a/b = 0.0585 (Side View)

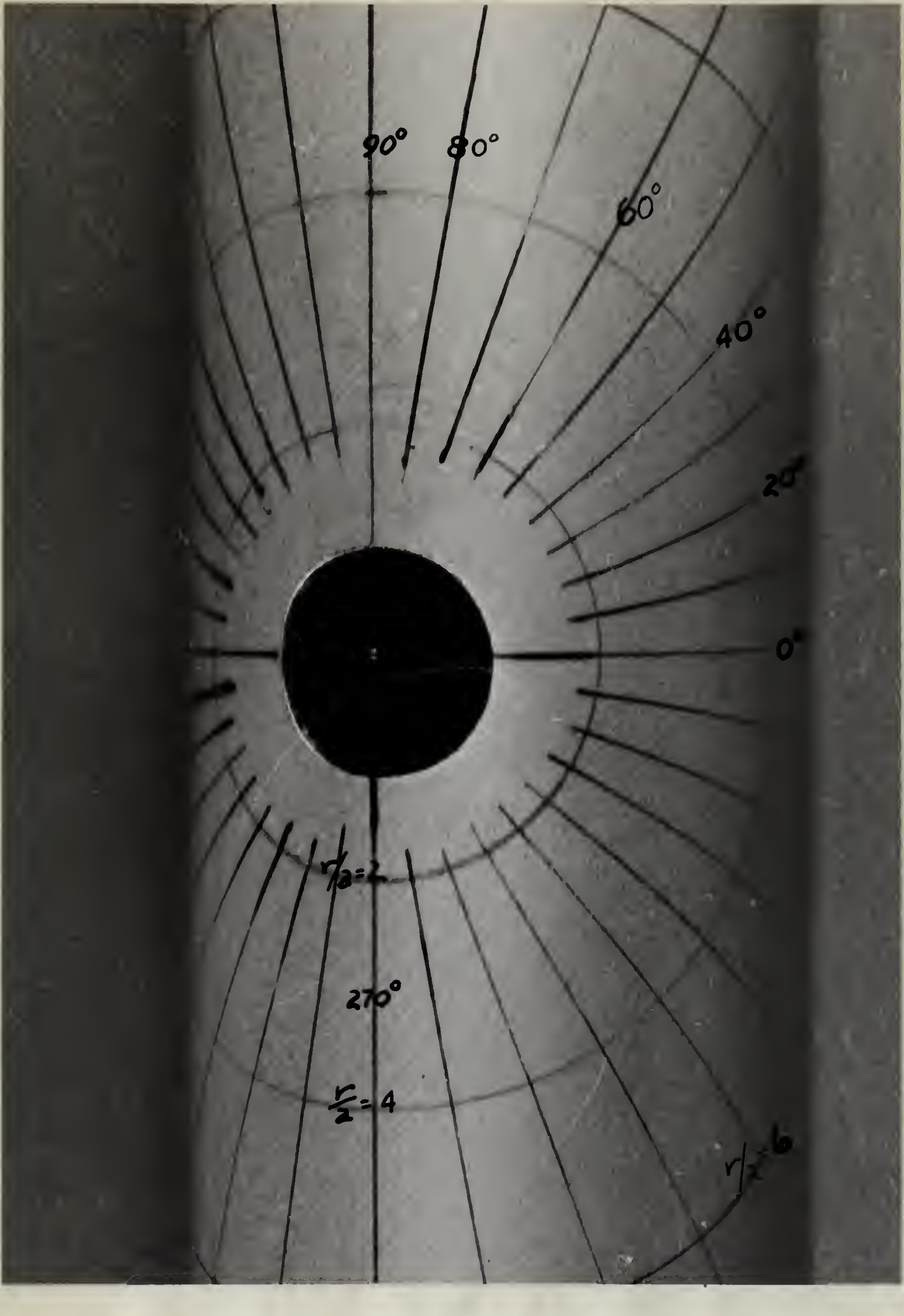

Fig. 9 Stresscoat Crack Pattern for a/b = 0.0585 (Top View)

Fig. 10 Stresscoat Crack Pattern for a/b = 0.106 (Side View)

[illegible] = [illegible]

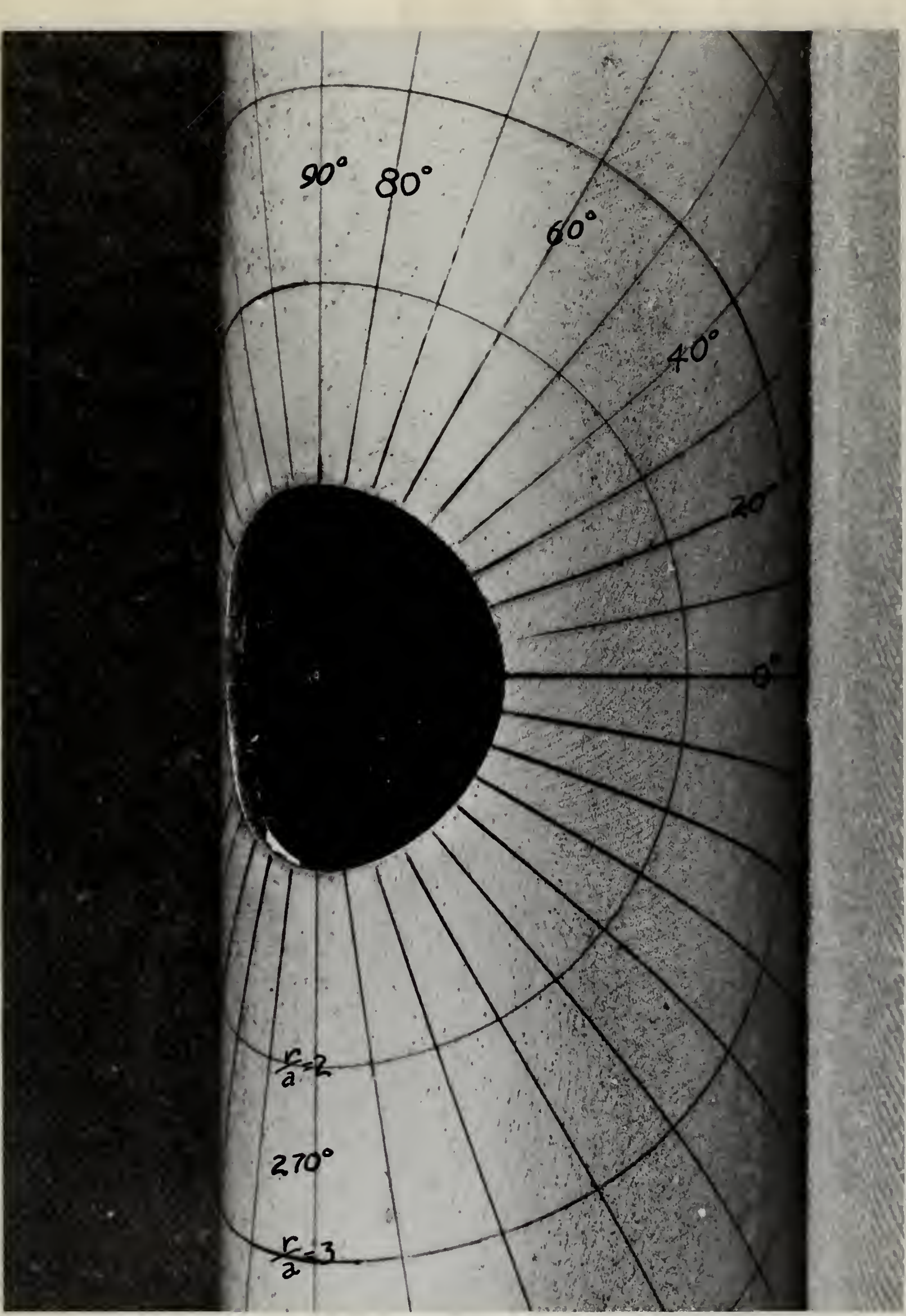

Fig. 11 Stresscoat Crack Pattern for a/b = 0.106 (Top View)

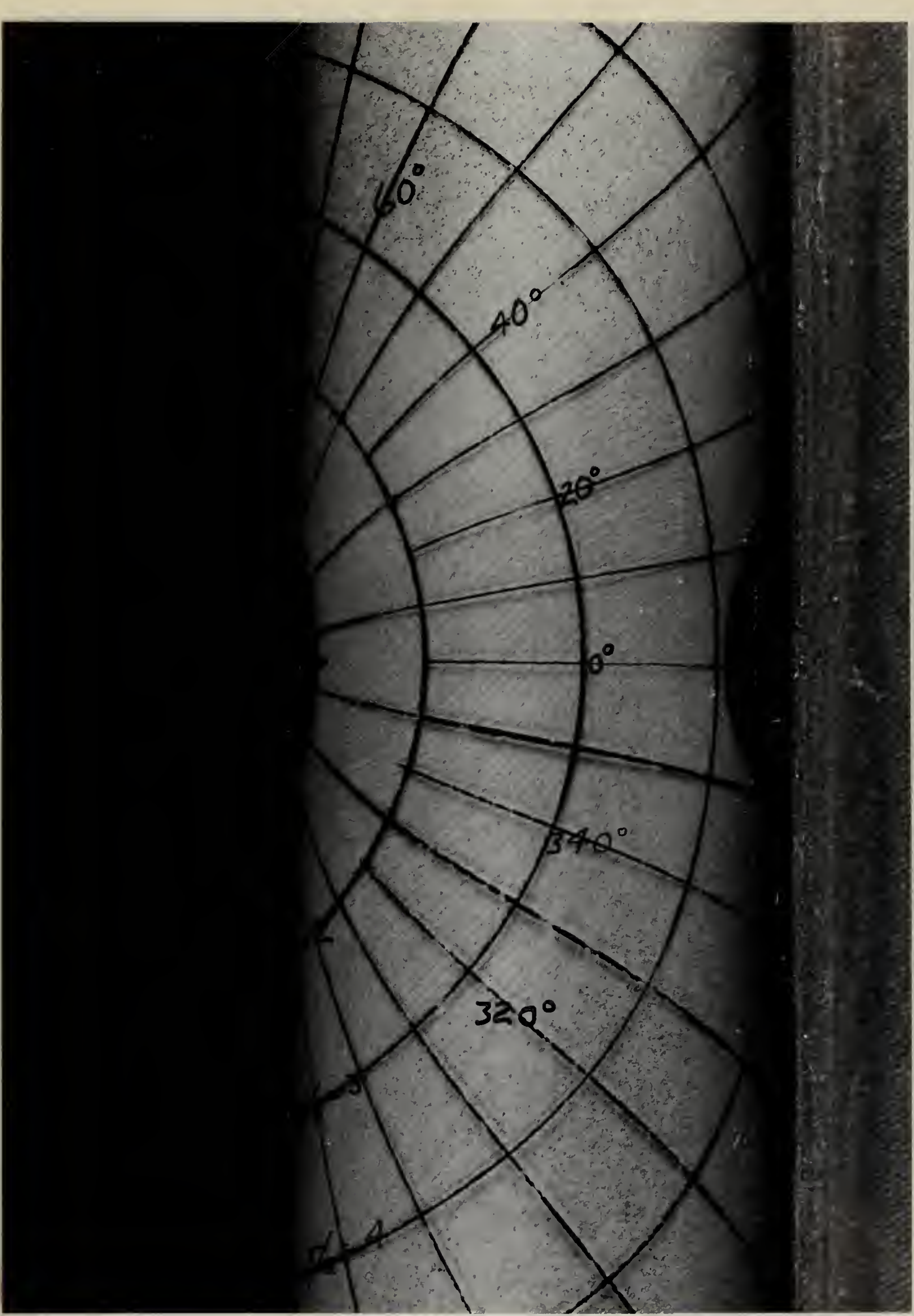

Fig. 12 Stresscoat Crack Pattern for a/b = 0.202 (Side View)

[illegible]

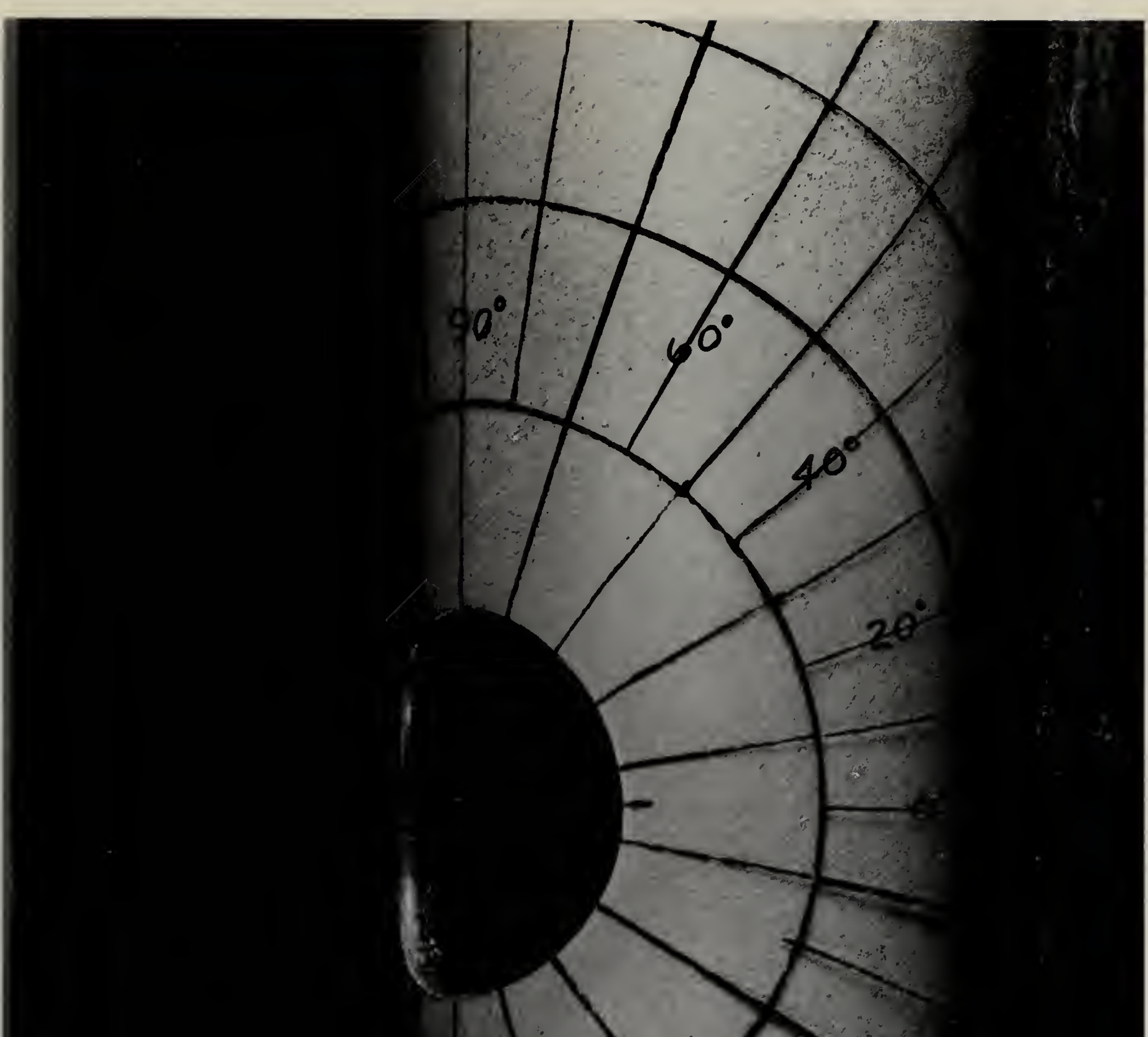

Fig. 13 Stresscoat Crack Pattern for a/b = 0.202 (Top View)

[illegible]

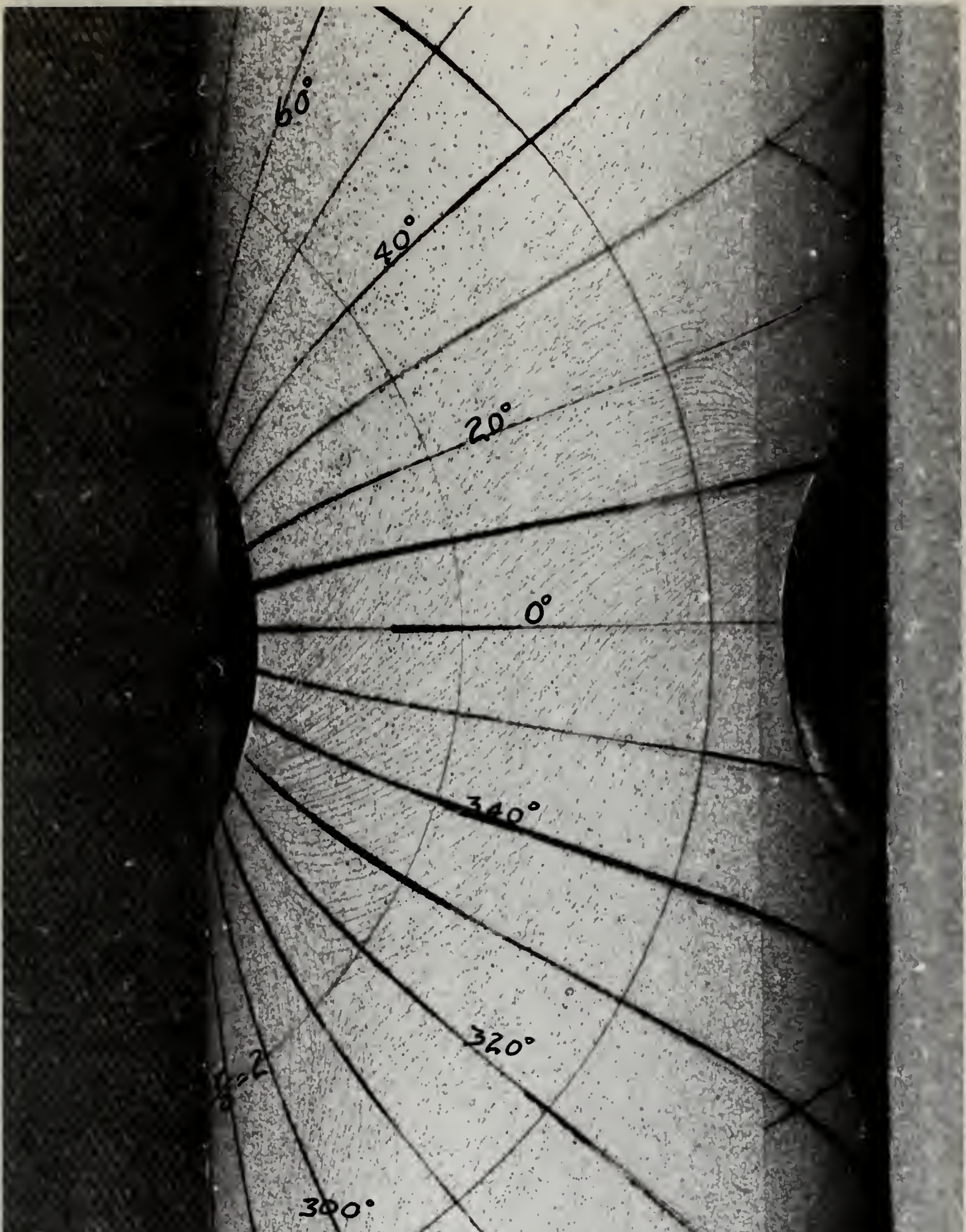

Fig. 14 Stresscoat Crack Pattern for a/b = 0.23 (Side View)

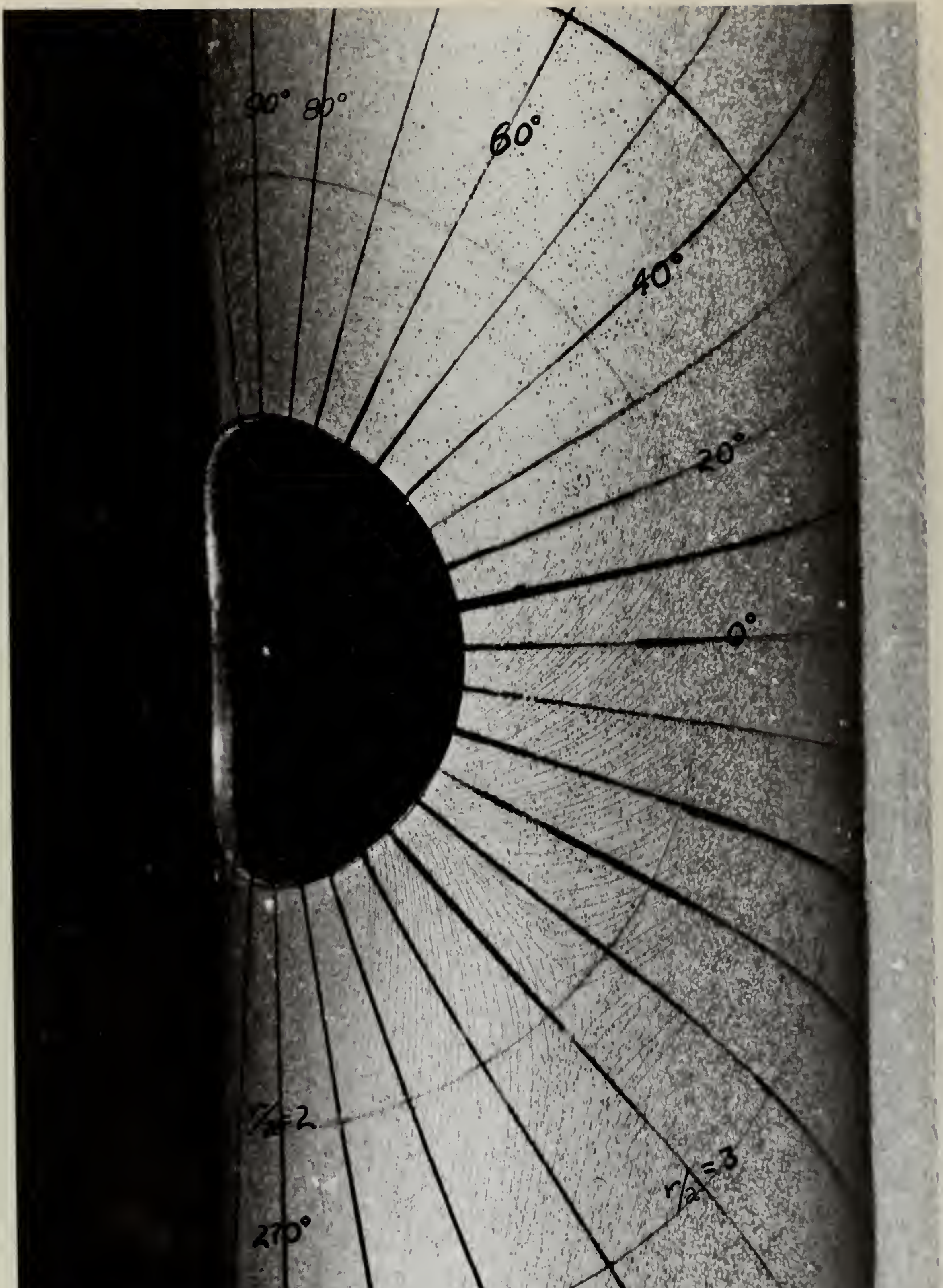

Fig. 15 Stresscoat Crack Pattern for a/b = 0.23 (Top View)

[illegible] = [illegible]

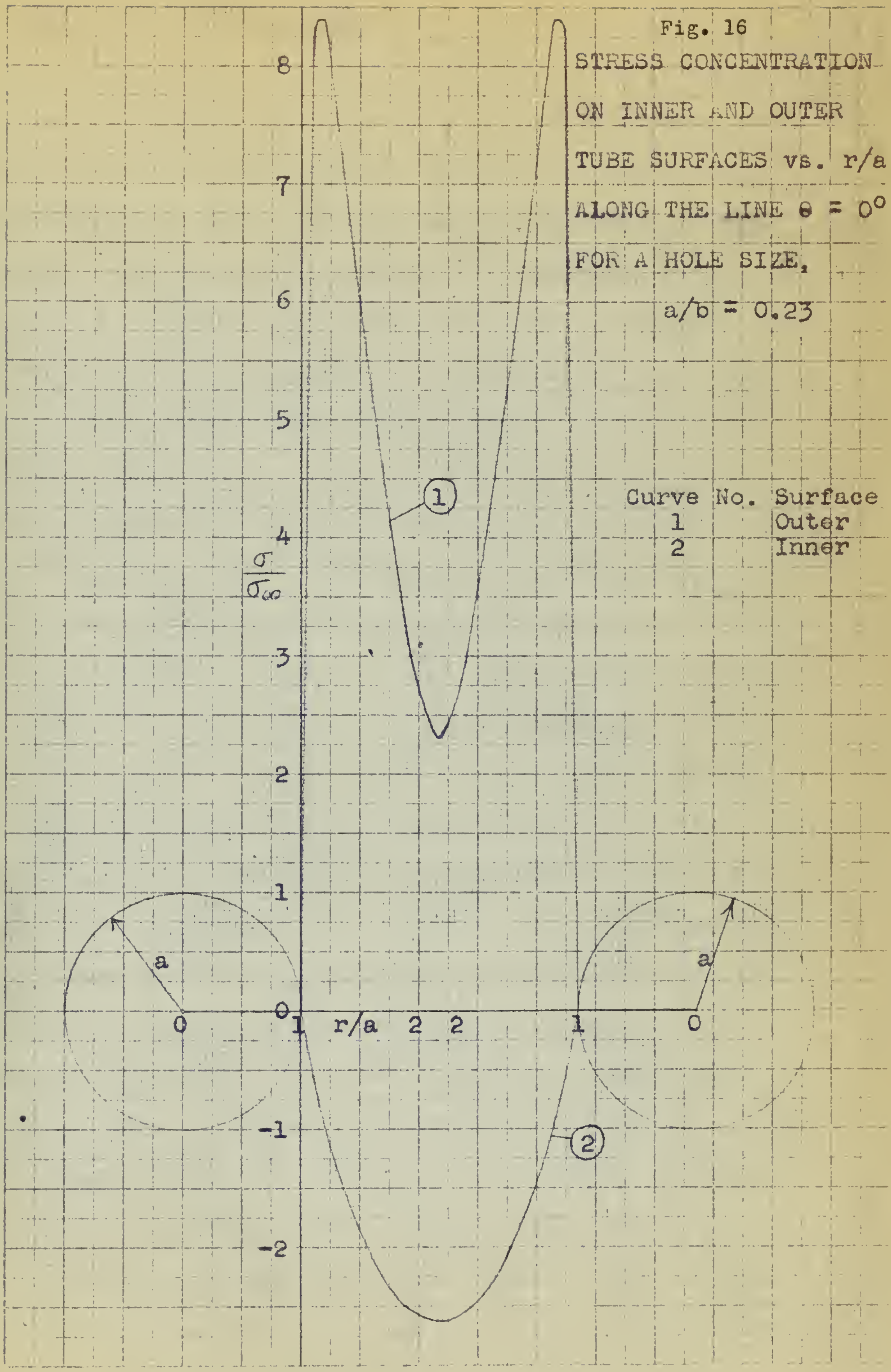

Fig. 16
STRESS CONCENTRATION
ON INNER AND OUTER
TUBE SURFACES vs. r/a
ALONG THE LINE $\theta = 0^\circ$
FOR A HOLE SIZE,
$a/b = 0.23$

19. Interpretation of results.

Fig. 4 shows that the stresses along the line $\theta = 0^\circ$ are extremely large in the immediate vicinity of the hole. The tube containing the holes with the largest a/b ratio (0.23) develops a stress concentration of 8.4 at a very short distance from the edge of the hole. The discontinuity of the tube surface resulting from the removal of the tube material at the hole serves to invoke a condition near the hole recognized as a combination of Saint Venant torsion and that torsion characterized by constant shear through the thickness of the tube. In this particular case, the stress induced as a result of the discontinuity of the tube sheet (Saint Venant's torsion) is predominant near the hole, and any attempt to establish correspondence between an anticipated simple, two-dimensional stress system and that actually obtained would be futile. To ascertain that this was truly the explanation for the magnitudes of the stresses obtained, strain gages were cemented on the inner surface of the tube along the same reference line, $\theta = 0^\circ$. It was found that the shear stresses were not constant through the thickness of the tube wall, but that the stress in a particular direction underwent a change in magnitude and in sign in transition from the outer tube surface to the inner surface. This is shown graphically in Fig. 16. A subsequent equilibrium check indicated that the fraction of the total torque carried by twisting of the sheet was small (about 15%). Nevertheless, the shearing stresses accompanying the twisting action are actually higher than those due to the other torsion phenomenon, so that the shearing stresses

are of opposite sign on the inside surface of the tube. It is apparent, too, that in each case, the stresses near the hole are not constant through the thickness of the tube, or in other words, the problem is not the simple, two-dimensional, plane problem previously foreseen. Only in the tube with the smallest a/b ratio are the stresses resulting from Saint Venant's torsion diminished sufficiently that one can see the rise of what was anticipated in the shape of the stress concentration curve (see Fig. 4).

20. Similarities to the Kirsch problem.

Due to the three-dimensional aspect of the tube problem, as indicated by the data secured, any comparison between the results obtained and the solution for an associated plane problem would seem to be useless. There are, however, two parallels between the stress distribution for the tube with an a/b ratio of 0.0585 and the theoretical solution for the single hole in the infinite plate which can be drawn from information supplied in Fig. 4 and in the Stresscoat crack patterns. The first was noted in the previous paragraph in which mention was made that a reasonable curve of stress concentration along the line $\theta = 0^\circ$ resulted at a distance from the hole at which the influence of the Saint Venant torsion was no longer pronounced. The second may be seen in the photographs (Figs. 8 and 9) along the line $\theta = -45^\circ$. Here, as in the theoretical solution for the single hole in an infinite plate, the principal stresses are oriented in the radial and tangential directions; $\sigma_1 = \sigma_r$; $\sigma_2 = \sigma_\theta$, i.e., $\sigma_r > \sigma_\theta$. As the a/b ratio is increased, each parallel vanishes, and the distribution of stresses becomes entirely different. An isotropic point appears at r/a = 2.1, $\theta = -45^\circ$; five degrees away

at $\theta = -40^\circ$, σ_θ is contractional immediately adjacent to the hole, but between the values of $r/a = 1.1$ to 1.9, $\sigma_\theta = \sigma_1$. (Recall that in the solution for the hole in the infinite plate $\sigma_\theta = \sigma_2$ along the line $\theta = -45^\circ$ for this system of loading.) Thus, it can be seen that except for the feature of anti-symmetry, this tube problem really has no close relation among the plane problems.

CHAPTER V

MAJOR SOURCES OF ERROR

21. Loading error.

A series of tests were conducted with AX-5 strain gages to determine whether the torsion tester applied a pure torque to a tube under test. It was found that a bending moment providing compression at the top surface of the tube was superimposed on the torque load. Percentagewise, the bending moment amounted to $2\frac{1}{2}$% of the torque. The primary loading reference strain gage data were not affected, because these gages were connected as their own active and compensating gages. Each test section was installed in the torsion tester with the hole in the topmost position. Note was taken of the presence of the bending stresses, but no attempt was made to correct any data for bending.

22. Uncertainties inherent in Stresscoat tests.

Some uncertainty exists first in selecting the proper strain threshold sensitivity value from the crack pattern on the calibration strip and, secondly, in matching Stresscoat cracks on the test specimen with those on the calibration strip. On the average, depending on the experience of the operator, this uncertainty may be assigned a value of 10%.

Further uncertainty arises from the use of only 4 calibration strips for each test, the duration of which ranged from 3 to 6 hours under varying temperature and humidity conditions.

> Quantitative error caused by difference in temperature between Calibration Strip and structure is approximately 10% per one degree F. [9]

It is probable, then, that some portions of the test data contained as much as 20% error (see Appendix I); however, strain gage data confirmed that Stresscoat data at the start and conclusion of tests was accurate within 10% (see Table 2). It is believed that an overall average of 15% could conservatively represent the error involved in the results.

TABLE 2

COMPARISON OF STRESSCOAT AND STRAIN GAGE DATA

	Location			*
a/b	r/a	θ	($\frac{\epsilon_1}{\epsilon_\infty}$)gage	($\frac{\epsilon_1}{\epsilon_\infty}$)Stresscoat
0.0585	2	0°	2.49	2.35
0.0585	3	0°	1.4	1.45
0.0585	3	0°	1.38	1.45
0.106	1.5	0°	5.92	5.9
0.106	3	35°	1.26	**
0.106	2	90°	2.2	2.15
0.106	4	90°	1.14	**
0.106	5	90°	1.09	**
0.23	1.5	0°	5.3	6.0
0.23	2	0°	2.68	2.6

* This column was obtained from several tests.

** These strain concentrations were established by the strain gage data, and no comparison can be realized.

CHAPTER VII

CONCLUSION

The most important conclusion which can be formed from an overall analysis of the data obtained is a recognition of the inadequacy of a theoretical, two-dimensional solution to predict the stress distribution in this tube problem. Had a theoretical solution been available and accepted, errors of the order of 100% to 200% (margin of error established by equilibrium checks) would have been sustained. Clearly, a discrepancy of this amount is important, especially if no prior knowledge of the magnitude of the error exists. On the other hand, it is believed that the results presented herein are accurate within 15%, a figure based upon equilibrium calculations and consistencies between Stresscoat data and strain gage data.

BIBLIOGRAPHY

1. Durelli, A.J., and T.N. DeWolf. Law of failure of Stresscoat. Proceedings of the Society for Experimental Stress Analysis VI-2:68, 1949.
2. Green, A.E. General biharmonic analysis for a plate containing circular holes. Proceedings of the Royal Society A 176:121, 1940.
3. Howland, R.C.J. Stress concentration due to a row of holes in a stretched plate. Proceeding of the Royal Society A 148:471, 1935.
4. Howland, R.C.J., and R.C. Knight. Stress functions for a plate containing groups of circular holes. Philosphic Transactions of the Royal Society A 238:357, 1940.
5. Hetenyi, M. Handbook of experimental stress analysis. New York, Wiley, 1950.
6. Hetenyi, M. and W.E. Young. Application of the brittle lacquer method in the stress analysis of machine parts. Proceedings of the Society for Experimental Stress Analysis I-2:126, 1944.
7. Jeffery, G.B. Plane stress and plane strain in bipolar coordinates. Philosophic Transactions of the Royal Society A 221:265, 1921.
8. Lourye, A.I. Concentration of stresses in the vicinity of an aperture in the surface of a circular cylinder. Prikladnaya Matematika i Mekhanika X:397, 1946.
9. Magnaflux Corporation. Stresscoat operating instructions.

10. Ruffner, et al. Stresses at cutouts in shear resistant webs as determined by the photoelastic method. Technical Note 984, Oct. 1945.

11. Timoshenko, S. and J.N. Goodier. Theory of elasticity. New York, McGraw-Hill, 1951.

12. Wang, C.K. Theoretical analysis of perforated shear webs. American Society of Mechanical Engineers. 13:A-77, 1946.

Fig. 17 STRAIN CONCENTRATION vs. r/a ALONG THE LINE θ = 25°

FOR A TUBE WITH A HOLE SIZE, a/b = 0.106

Note: This illustration is shown to indicate the method employed in obtaining strain concentration curves and to indicate the degree of accuracy which may be expected in these tests with brittle lacquer.

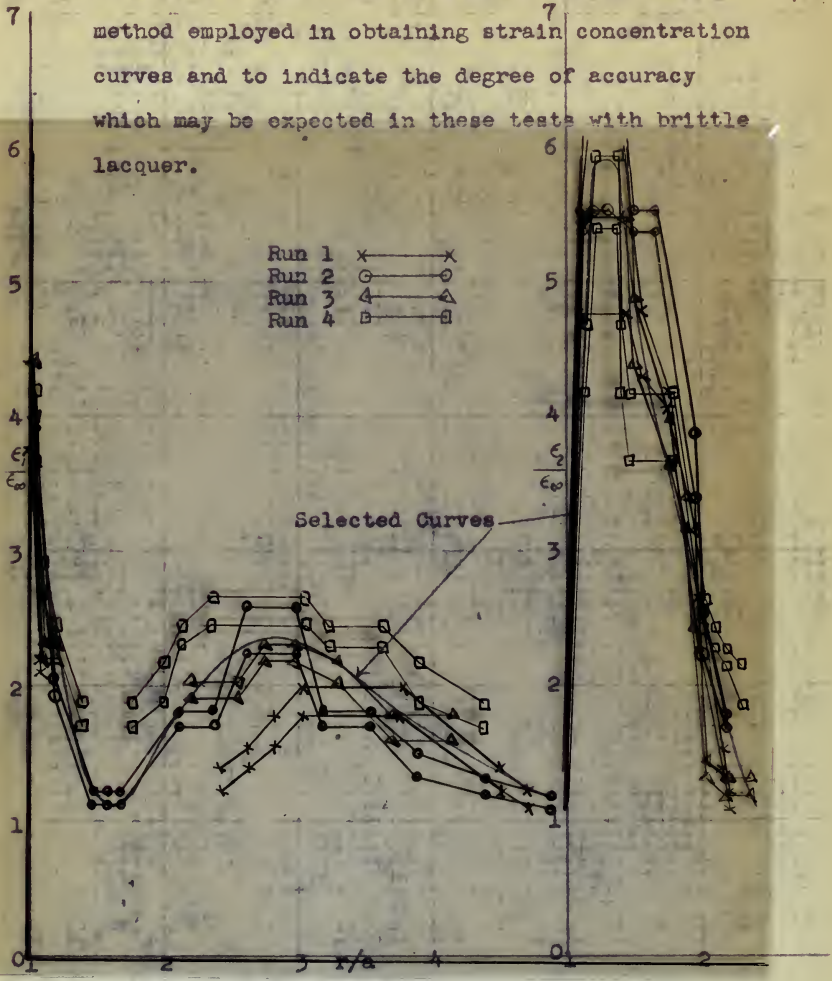

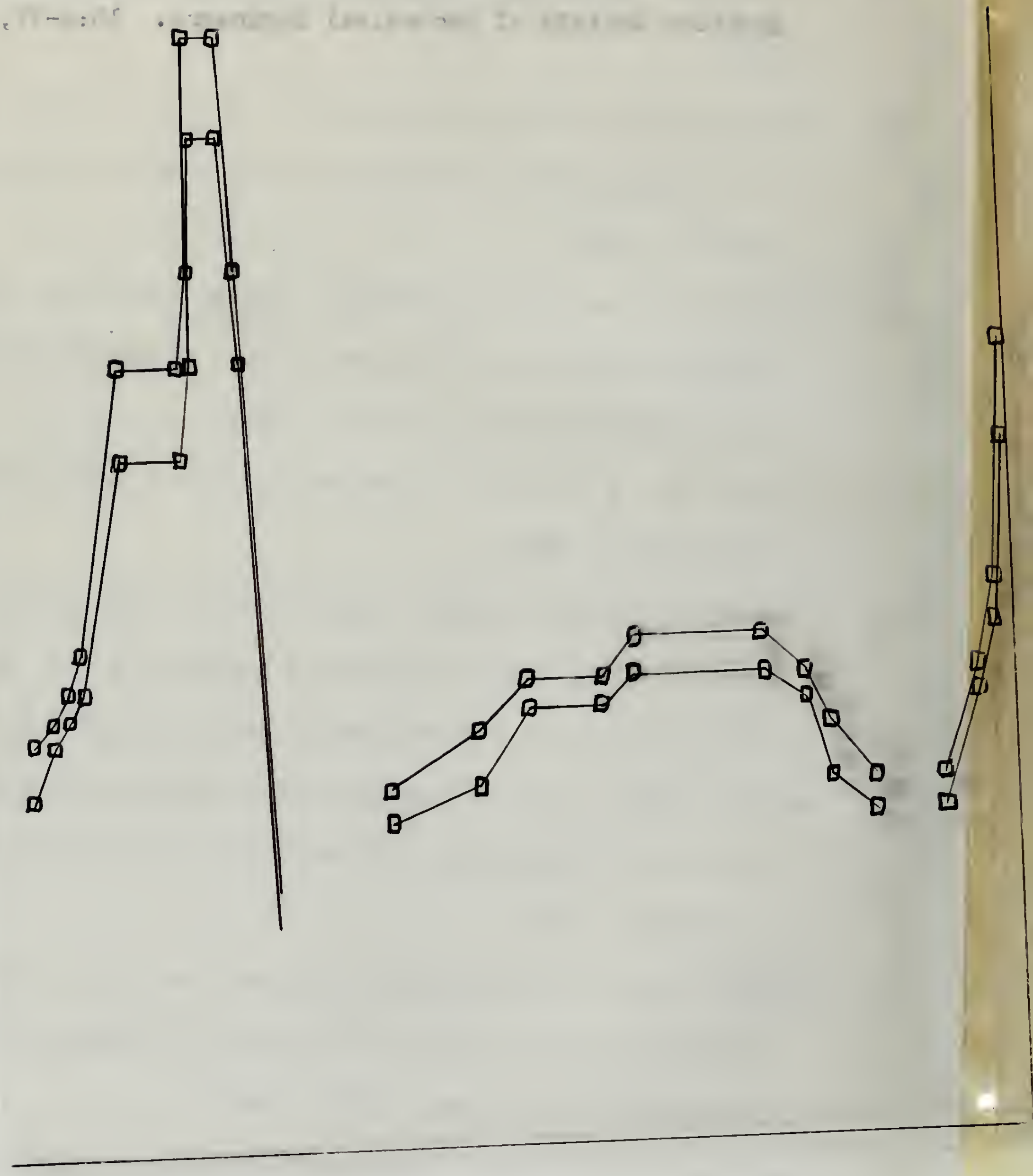

17 STRAIN CONCENTRATION vs. r/a ALONG THE LINE $\theta = 25^\circ$ FOR A TUBE WITH A HOLE SIZE, $a/b = 0.106$

Note: This illustration is shown to indicate the method employed in obtaining strain concentration curves and to indicate the degree of accuracy which may be expected in these tests with brittle lacquer.

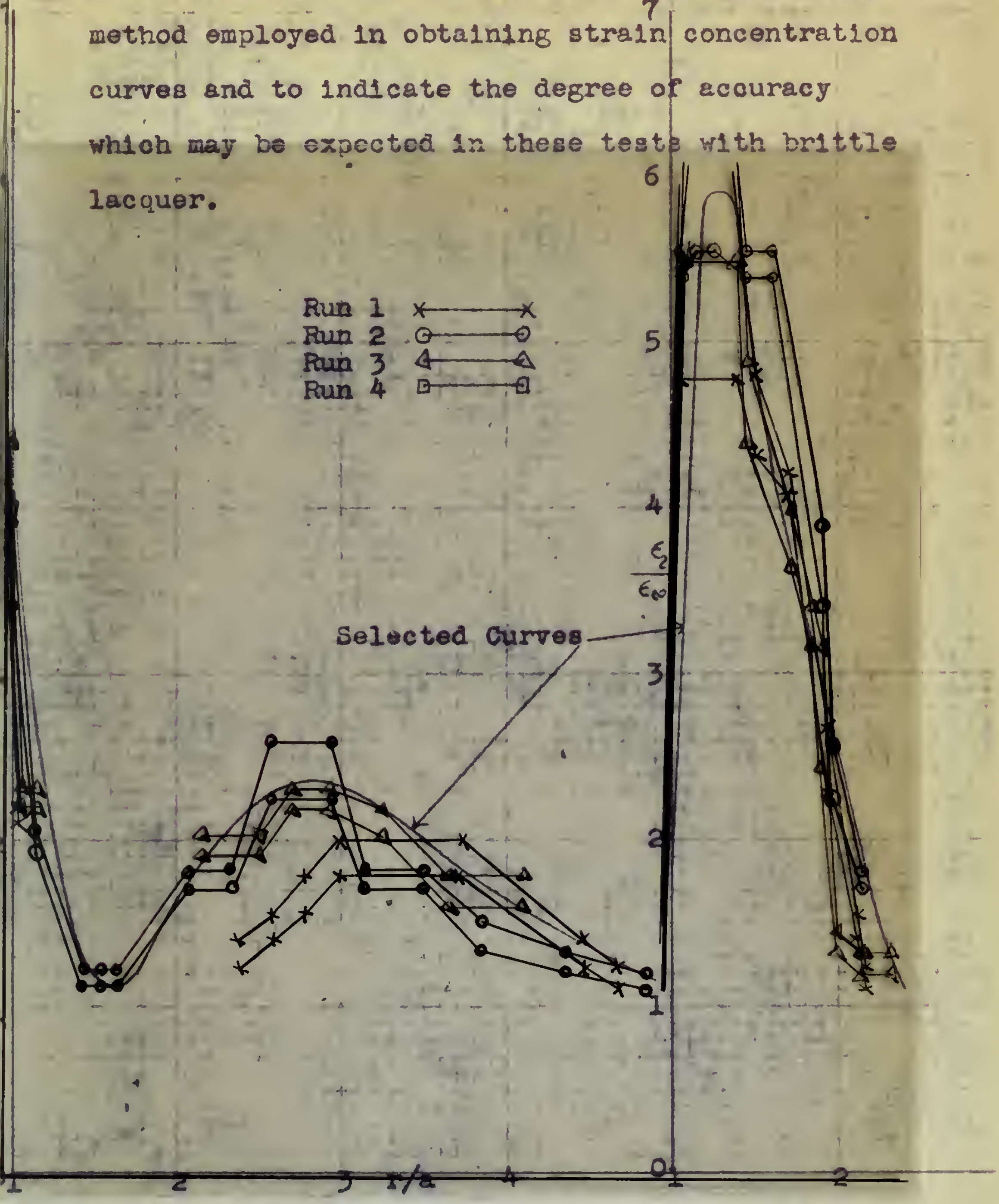

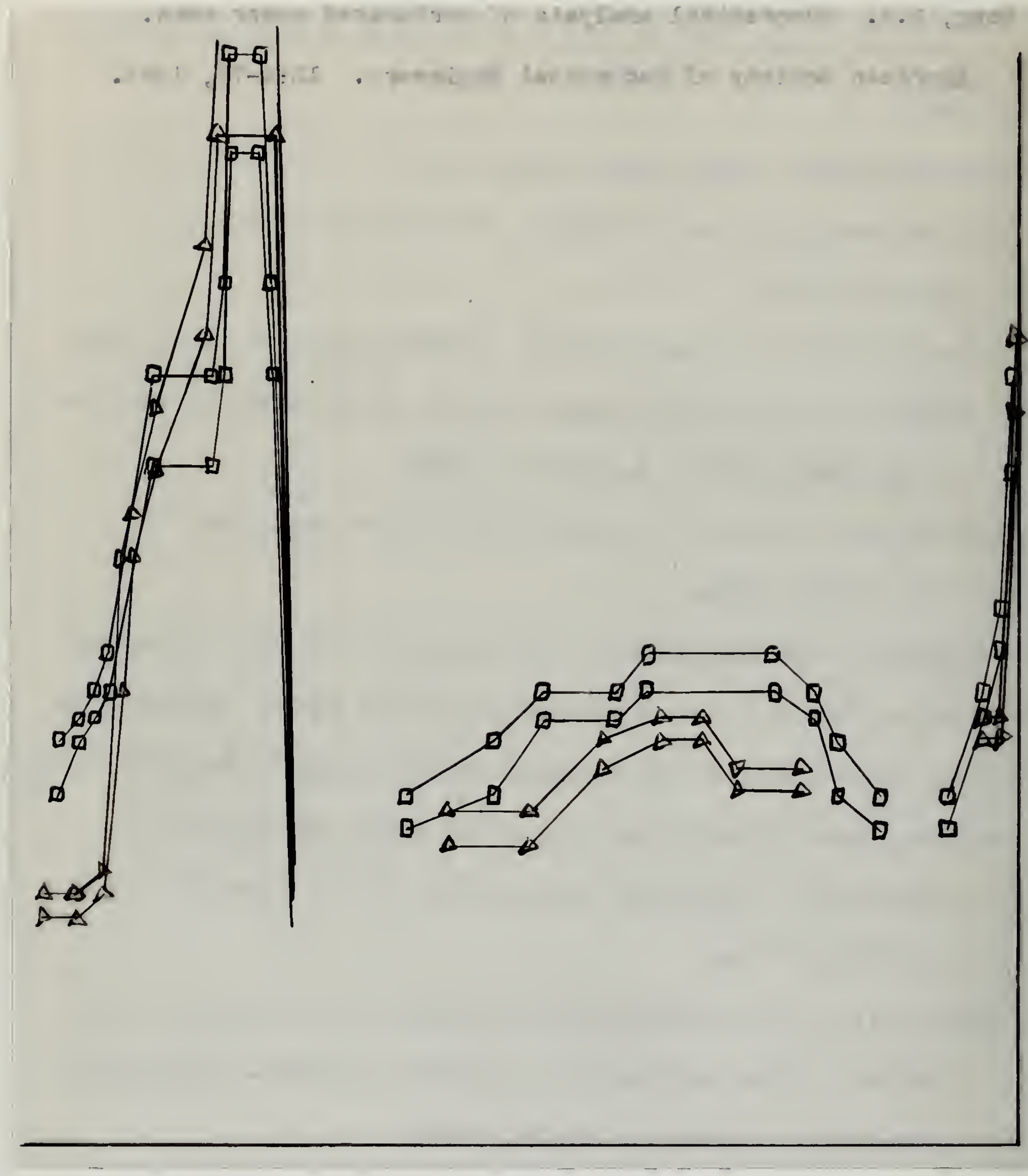

Appendix I

Fig. 17 STRAIN CONCENTRATION vs. r/a ALONG THE LINE $\theta = 25^\circ$ FOR A TUBE WITH A HOLE SIZE, $a/b = 0.106$

Note: This illustration is shown to indicate the method employed in obtaining strain concentration curves and to indicate the degree of accuracy which may be expected in these tests with brittle lacquer.

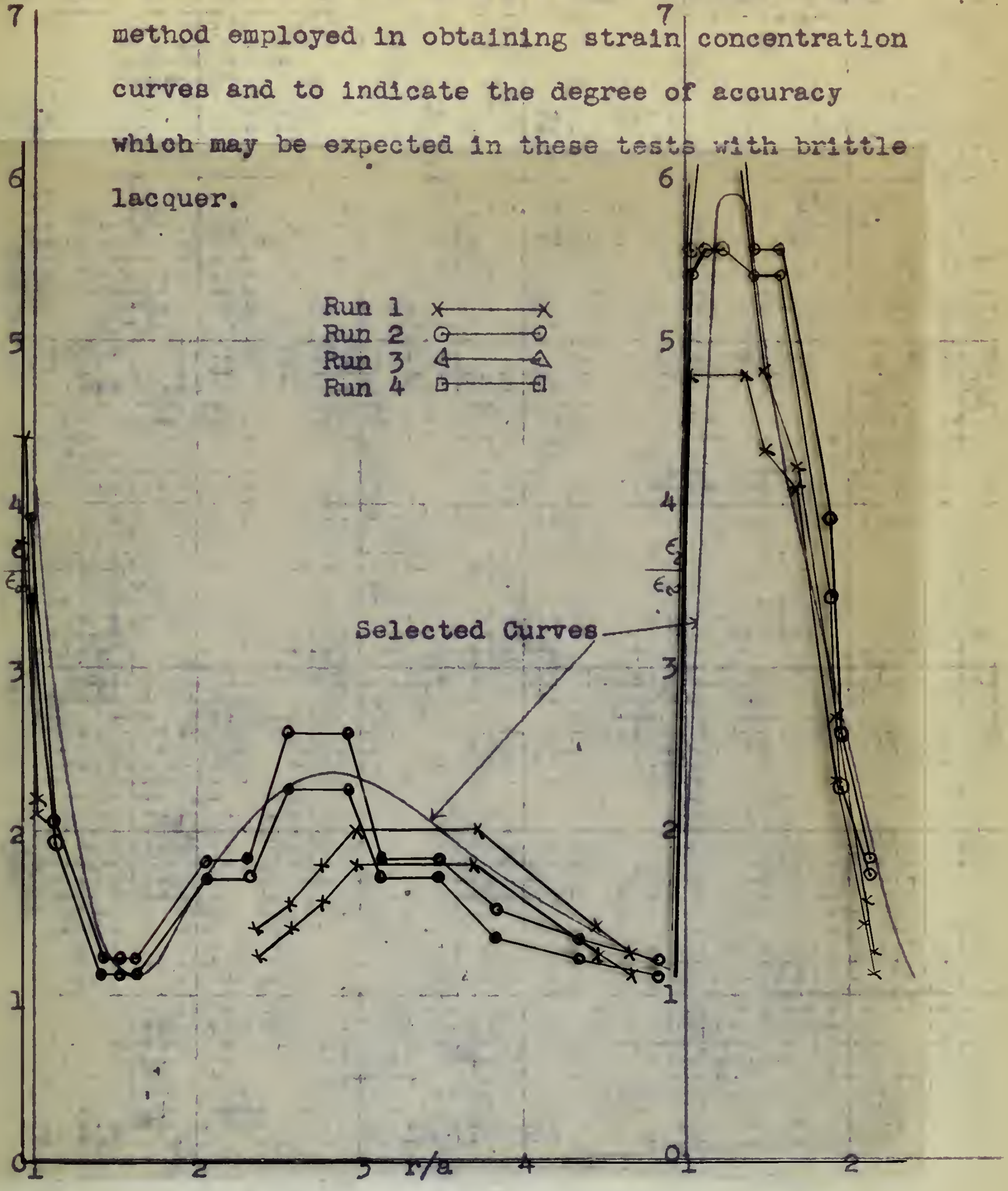

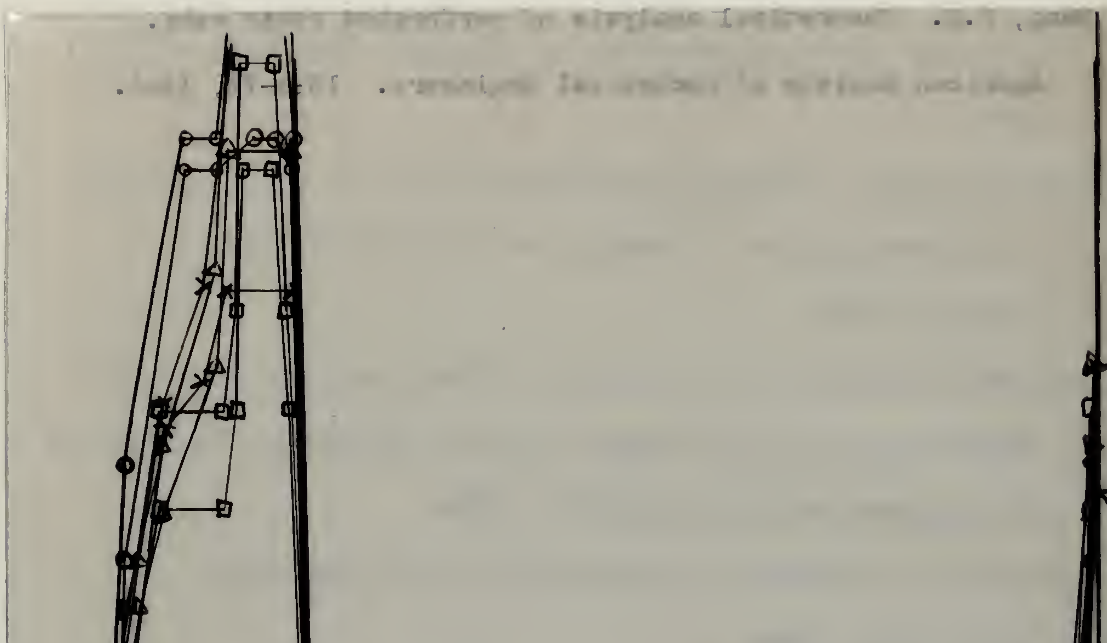

ig. 17 STRAIN CONCENTRATION vs. r/a ALONG THE LINE $\theta = 25^\circ$

FOR A TUBE WITH A HOLE SIZE, $a/b = 0.106$

Note: This illustration is shown to indicate the method employed in obtaining strain concentration curves and to indicate the degree of accuracy which may be expected in these tests with brittle lacquer.

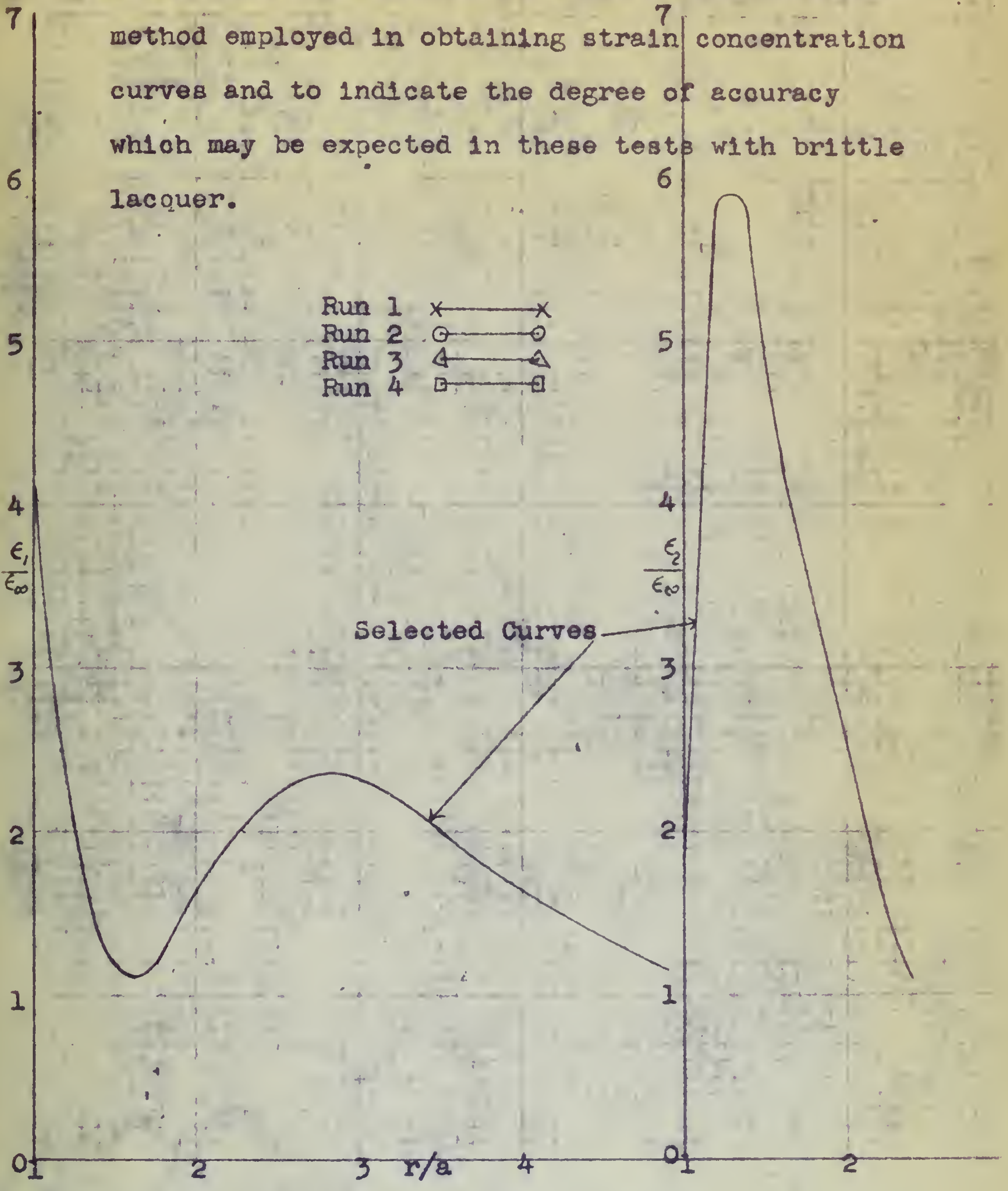

Appendix II

Proof that the Tube with a Single Hole Has No Analogue among the Plane Problems

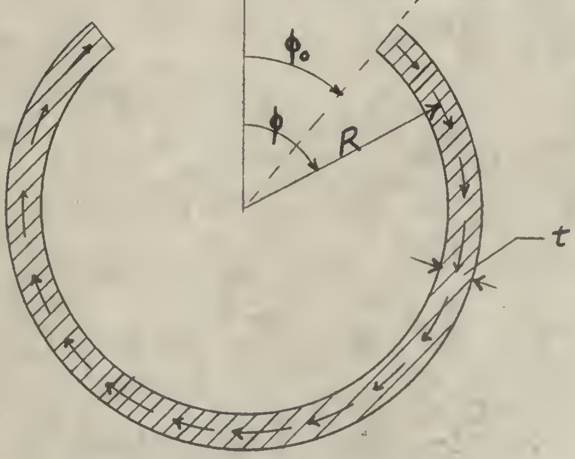

Fig. 18. Right Circular Cross-section of Tube Taken on a Plane through the Center of the Hole.

It is assumed that the shearing stress (τ) is constant through the thickness of the tube. The condition of static equilibrium which requires that the horizontal forces vanish has no counterpart among the plane problems. This condition is:

$$\int_{\phi_0}^{2\pi-\phi_0} \tau t R \, d\phi \cos\phi = 0$$

or

$$\int_{\phi_0}^{\pi} \tau t R \, d\phi \cos\phi = 0$$

It is apparent that no plane problem can be analogous to the tube with a single hole, since in no case can a comparable plane problem be found in which the equations of static equilibrium contain a cos ϕ factor.

Thesis Mayes 20647
M393 Stresses near a hole in a tube under torsion.